

Recent Developments on PIXE Simulation with Geant4

M. G. Pia, G. Weidenspointner, M. Augelli, L. Quintieri, P. Saracco, M. Sudhakar, and A. Zoglauer

Abstract—Particle induced X-ray emission (PIXE) is an important physical effect that is not yet adequately modelled in Geant4. This paper provides a critical analysis of the problem domain associated with PIXE simulation and describes a set of software developments to improve PIXE simulation with Geant4. The capabilities of the developed software prototype are illustrated and applied to a study of the passive shielding of the X-ray detectors of the German eROSITA telescope on the upcoming Russian *Spectrum-X-Gamma* space mission.

Index Terms—Monte Carlo, Geant4, PIXE, ionization.

I. INTRODUCTION

THE application of particle induced X-ray emission (PIXE) to non-destructive trace element analysis of materials has first been proposed by Johansson and co-workers in 1970 [1]. Today, this experimental technique is widely exploited in diverse fields [2].

The physical process of PIXE may also give rise to unwanted instrumental background X-ray lines, as is the case for space missions and for some laboratory environments. It also affects the spatial distribution of the energy deposit associated with the passage of charged particles in matter: in this respect, its effects may become significant in the domain of microdosimetry.

The wide application of this experimental technique has motivated the development of several dedicated software systems; nevertheless, despite its large experimental interest, limited functionality for PIXE simulation is available in general-purpose Monte Carlo codes.

This paper discusses the problem of simulating PIXE in the context of a general-purpose Monte Carlo system and describes a set of developments to improve its simulation with Geant4 [3], [4]. Finally, it illustrates an application of the developed PIXE simulation prototype to the optimization of

the passive shield of the X-ray detectors of the eROSITA [5] (extended Roentgen Survey with an Imaging Telescope Array) telescope on the *Spectrum-X-Gamma* [6] space mission.

II. SOFTWARE FOR PIXE: AN OVERVIEW

Software tools are available in support of PIXE experimental applications as specialized codes or included in general-purpose simulation systems.

A. Specialized PIXE codes

Dedicated PIXE codes are focussed on the application of this technique to elemental analysis. They are concerned with the calculation of experimentally relevant X-ray yields resulting from the irradiation of a material sample by an ion beam: primarily transitions concerning the K shell, and in second instance transitions originating from vacancies in the L shell.

For this purpose various analysis programs have been developed, which are able to solve the inverse problem of determining the composition of the sample from an iterative fitting of a PIXE spectrum; some among them are GeoPIXE [7], GUPIX [8]–[10], PIXAN [11], PixeKLM [12], Sapix [13], WinAxil [14] and Wits-HEX [15]. A few codes concern PIXE simulation [16]–[18] specifically.

These codes share basic physics modelling options, like the adoption of the ECPSSR (Energy-Loss Coulomb-Repulsion Perturbed Stationary State Relativistic) [19] model for the calculation of ionization cross sections; they handle simple experimental geometries, such as target materials consisting of layers, and impose limitations on the type of samples that can be analyzed.

B. PIXE simulation in general-purpose Monte Carlo systems

Dedicated PIXE software systems have a limited application scope, as they lack the capability of dealing with complex experimental configurations.

Comprehensive modelling capabilities are usually associated with general-purpose Monte Carlo systems. However, the simulation of PIXE is not widely covered by large scale Monte Carlo codes treating hadron interactions, while the conceptually similar simulation of electron impact ionisation is implemented in the EGS [20]–[22] and Penelope [23] electron-photon Monte Carlo systems. The Geant4 simulation toolkit addresses X-ray emission induced both by electrons and heavy particles like protons and α particles.

The physics that needs to be considered for the simulation of PIXE includes the energy loss and scattering of the incident

Manuscript received April 3, 2009.

Maria Grazia Pia and Paolo Saracco are with INFN Sezione di Genova, Via Dodecaneso 33, 16146 Genova, Italy (e-mail: MariaGrazia.Pia@ge.infn.it, Paolo.Saracco@ge.infn.it).

Georg Weidenspointner is with the Max-Planck-Institut für extraterrestrische Physik, Postfach 1603, 85740 Garching, Germany, and with the MPI Halbleiterlabor, Otto-Hahn-Ring 6, 81739 München, Germany (e-mail: Georg.Weidenspointner@hll.mpg.de).

Mauro Augelli is with the Centre d'Etudes Spatiales (CNES), 18 Av. Edouard Belin, 31401 Toulouse, France (e-mail:mauroaugelli@mac.com).

Lina Quintieri is with INFN Laboratori Nazionali di Frascati, Via E. Fermi 40, I-00044 Frascati, Italy (e-mail: Lina.Quintieri@lnf.infn.it).

Manju Sudhakar is with INFN Sezione di Genova, Via Dodecaneso 33, 16146 Genova, Italy (e-mail:Manju.Sudhakar@ge.infn.it) and Phys. Dept., Univ. of Calicut, India; she is on leave from ISRO, Bangalore, India.

Andreas Zoglauer is with the Space Sciences Laboratory, University of California at Berkeley, 7 Gauss Way, Berkeley, CA 94720, USA (e-mail: zog@ssl.berkeley.edu).

charged particle, atomic shell ionization cross sections, and atomic transition probabilities and energies. On top of these physics features, consistency should be ensured, when modelling PIXE, with the particle transport schemes governing the Monte Carlo simulation.

Intrinsically, PIXE is a discrete process: X-ray emission occurs as the result of producing a vacancy in atomic shell occupancy, in competition with Auger electron emission and Coster-Kronig transitions. Nevertheless, this discrete process is intertwined with the ionization process, which determines the production of the vacancy; this process, for reasons which are elucidated below, is treated in general-purpose Monte Carlo codes with mixed condensed and discrete transport schemes. The transport scheme to which ionization is subject affects the simulation of PIXE.

The simulation of the energy loss of a charged particle due to ionization is affected by the infrared divergence of the cross section for producing secondary electrons. In the context of general purpose Monte Carlo systems, a discrete treatment of each individual ionization process becomes inhibitive, since, due to their large number, the required computation time becomes excessive.

Infrared divergence is usually handled in general-purpose Monte Carlo codes by adopting a condensed-random-walk scheme [24] for particle transport. In such a scheme, the particle's energy loss and deflection are treated as averaged net effect of many discrete interactions along the step, thereby substituting in the simulation a single continuous process for the many discrete processes that actually occur. In a mixed scheme, like the one adopted by Geant4 [3], two different régimes of particle transport are introduced, which are distinguished through a secondary production threshold setting, i.e. a threshold for the kinetic energy of the electron that is kicked out of an atom as a result of ionization (the so-called δ -ray): all ionizations that would generate δ -rays below the threshold are treated as a continuous process along the step, while the ionizations that produce δ -rays above the threshold are treated as a discrete process.

While this combined condensed-random-walk and discrete particle transport scheme is conceptually appealing and appropriate to many simulation applications, it suffers from drawbacks with respect to the generation of PIXE.

One drawback is that atomic relaxation occurs only in connection with the discrete part of the transport scheme, where the event of producing a δ -ray can be associated with the creation of a vacancy in the shell occupancy. For the same reason, the fluorescence yield depends on the threshold for the kinetic energy of the secondary electron.

Another drawback of the current transport scheme is that the cross section for discrete hadron ionization, i.e. for production of a δ -ray, is calculated from a model for energy loss that is independent of the shell where the ionization occurs. While theoretical calculations are available to determine the spectrum of the emitted electron for each sub-shell in the case of electron impact ionization [25] for any element, to the authors' knowledge no such facilities are currently available for the ionization induced by protons and ions. Experimental data are not adequate either to complement the lack of theoretical

calculations.

III. DEVELOPMENTS FOR PIXE SIMULATION WITH GEANT4

At the present time, the Geant4 toolkit does not provide adequate capabilities for the simulation of PIXE in realistic experimental use cases.

The first development cycle [26]–[29] had a limited scope: the implementations concerned only PIXE induced by α particles and involving K shell ionization - apart from the implementation based on Gryzinski's [30], [31] theoretical model, which produces physically incorrect results. Even with the models which calculate K shell ionization cross sections correctly, inconsistencies arise in the simulation of PIXE related to the algorithm implemented for determining the production of a K shell vacancy. The deficiencies exhibited by the software released in Geant4 9.2 [32] did not contribute to improve PIXE simulation with respect to the previous version.

A set of developments for PIXE simulation is described in the following sections. A preliminary overview of their progress was reported in [33].

The physics aspects associated with PIXE involve the creation of a vacancy in the shell occupancy due to ionization, and the emission of X-rays from the following atomic deexcitation. The former requires the knowledge of ionization cross sections detailed at the level of individual shells: for this purpose several models have been implemented and validated against experimental data. The latter exploits the existing functionality of Geant4 Atomic Relaxation package [34].

The domain decomposition at the basis of PIXE simulation with Geant4 identified three main entities with associated responsibilities: the hadron ionization process, the creation of a vacancy in the shell occupancy resulting from ionisation, the deexcitation of the ionised atom with the associated generation of X-rays. The simulation of PIXE is the result of the collaboration of these entities. A class diagram in the Unified Modelling Language (UML) [35] illustrates the main features of the software design in Fig. 1.

A. Ionisation cross section models

The simulation of PIXE concerns a variety of experimental applications, that require the capability of calculating ionisation cross sections over an extended energy range: from a few MeV typical of material analysis applications to hundreds MeV or GeV range of astrophysical applications.

Various theoretical and empirical models are available in literature to describe ionisation cross sections for different interacting particles, as well as compilations of experimental data. However, there is limited documentation in literature of systematic, quantitative assessments of the accuracy of the various models.

The current software prototype has adopted the strategy of providing an extensive collection of ionisation cross section models as a function of element, atomic (sub-)shell, and incident particle kinetic energy.

According to the chosen strategy, the provision of a cross section model is reduced to the construction of tabulations of

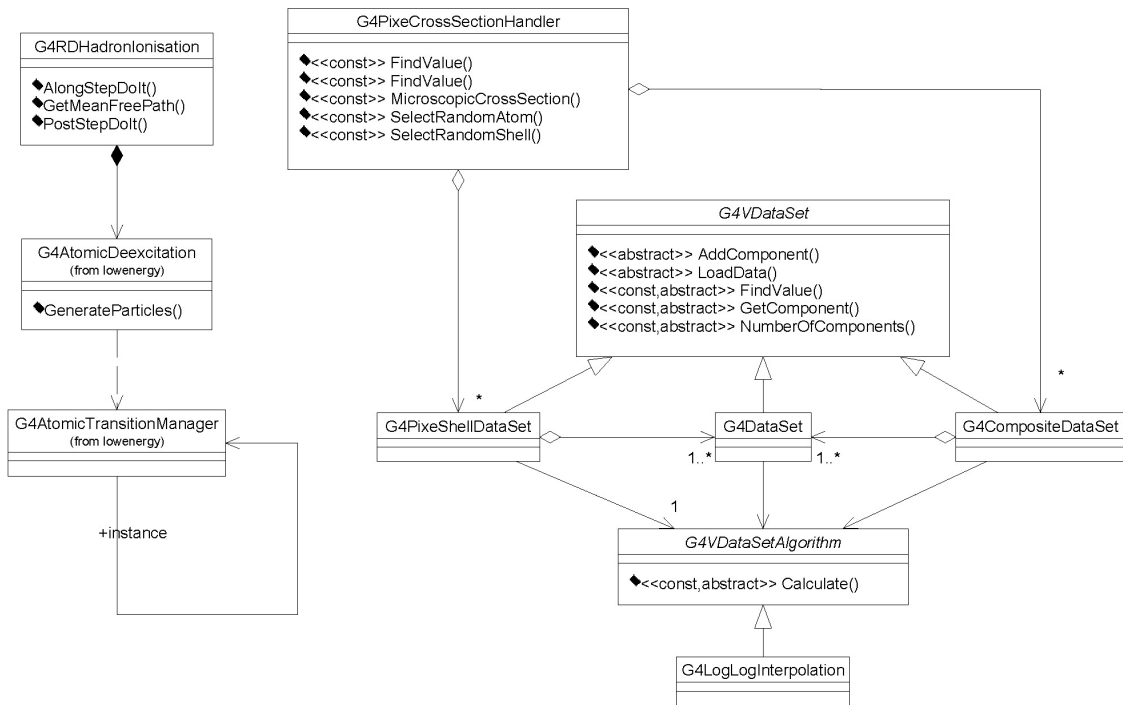


Fig. 1. The Unified Modelling Language class diagram of the developments for PIXE simulation described in this paper, illustrating the main features of the software.

its values at preset energies. The cross sections associated with the models described in this paper have been pre-calculated either using existing software documented in literature, or developing ad hoc code. The data are stored in files, which make up a data library for PIXE simulation with Geant4 - but could be used also by other codes. The cross section data sets selected by the user are loaded into memory at runtime; cross section values at a given energy are calculated by interpolation over the tabulated values whenever required.

The adopted data-driven approach for the provision of ionization cross sections presents various advantages. It optimizes performance speed, since the calculation of the interpolation is faster than the calculation from complex algorithms implementing theoretical models. This approach also offers flexibility: choosing a cross section model simply amounts to reading the corresponding set of data files; adding a new set of cross sections simply amounts to providing the corresponding set of data files, which are handled transparently. Finally, the cross section data are transparent to the user: the files are accessible to the user and human readable.

A wide choice of cross section models for K, L and M shell ionization is provided in the prototype software for protons and α particles. The availability of ionization cross section calculations and experimental data for outer shells is very limited in literature. Theoretical cross section models include Plane Wave Born Approximation (PWBA) and variants of the ECPSSR model: the original ECPSSR formulation [19], ECPSSR with United Atom correction (ECPSSR-UA) [36], ECPSSR with corrections for the Dirac-Hartree-Slater nature of the K shell [37] (ECPSSR-HS), as well as calculations based on recent improvements to K shell cross section specific

to high energy [38] (ECPSSR-HE).

The cross sections have been tabulated and assembled in a data library; the values at a given energy are calculated by interpolation. The tabulations corresponding to theoretical calculations span the energy range between 10 keV and 10 GeV; empirical models are tabulated consistently with their energy range of validity. The adopted data-driven approach optimizes performance speed and offers flexibility for choosing a cross section model.

ECPSSR tabulations have been produced using the ISICS software [39], [40], 2006 version and an extended version [41] including recent high energy developments. Tabulations of ECPSSR calculations as reported in [42] are also provided.

Empirical cross section models for K shell ionization include the tabulations for protons documented in [42] and a more recent one [43]. An empirical cross section model for K shell ionization by α particles is based on the tabulations in [44]. Empirical models for L shell ionization by protons have been developed by Miyagawa et al. [45], Sow et al. [46] and Orlic et al. [47].

The ISICS software allows the calculation of cross sections for heavier ions as well; therefore, the current PIXE simulation capabilities can be easily extended in future development cycles.

B. Generation of a vacancy

The determination of which atomic (sub-)shell is ionised is related to its ionisation cross section with respect to the total cross section for ionising the target atom. However, as previously discussed, the condensed-random-walk scheme

raises an issue as to estimating the total ionisation cross section at a given energy of the incident particle.

A different algorithm has been adopted with respect to the one implemented in the first development cycle: the vacancy in the shell occupancy is determined based on the total cross section calculated by summing all the individual shell ionisation cross sections. This algorithm provides a correct distribution of the produced vacancies as long as ionisation cross sections can be calculated for all the atomic shells involved in the atomic structure of the target element. Since cross section models are currently available for K, L and M shells only, at the present status of the software this algorithm overestimates PIXE for elements whose atomic structure involves outer shells, because of the implicit underestimation of the total ionization cross section. This approach, however, provides better control on the simulation results than the algorithm implemented in the first development cycle.

The production of secondary particles by the atomic relaxation of an ionized atom is delegated to the Atomic Relaxation component.

IV. SOFTWARE VALIDATION

The availability of a wide variety of cross section models for the first time in the same computational environment allowed a detailed comparative assessment of their features against experimental data.

The comparison of cross sections as a function of energy was performed for each element by means of the χ^2 test. Contingency tables were built on the basis of the outcome of the χ^2 test to determine the equivalent, or different behavior of model categories. The input to contingency tables derived from the results of the χ^2 test: they were classified respectively as “pass” or “fail” according to whether the corresponding p-value was consistent with a 95% confidence level. The contingency tables were analyzed with Fisher exact test [48].

A. K shell ionization cross sections

The reference experimental data were extracted from [42]. An example of how the simulation models reproduce experimental measurements is shown in Fig. 2.

The fraction of test cases for which the χ^2 test fails to reject the null hypothesis at the 95% and 99% confidence level are listed in Table I: all the cross section models implemented in the simulation exhibit equivalent behaviour regards the compatibility with the experimental data, with the exception of the Kahoul et al. model. The contingency table comparing the Kahoul et al. and ECPSSR-HS models confirms that the two models show a statistically significant difference regards their accuracy (p-value of 0.001).

The contingency tables associated with the other models show that they are statistically equivalent regarding their accuracy. However, when only the lower energy range (below 5-7 MeV, depending on the atomic number) is considered, a statistically significant difference at the 95% confidence level (p-value of 0.034) is observed between the ECPSSR model and the ECPSSR-HS one; the latter is more accurate with respect to experimental data.

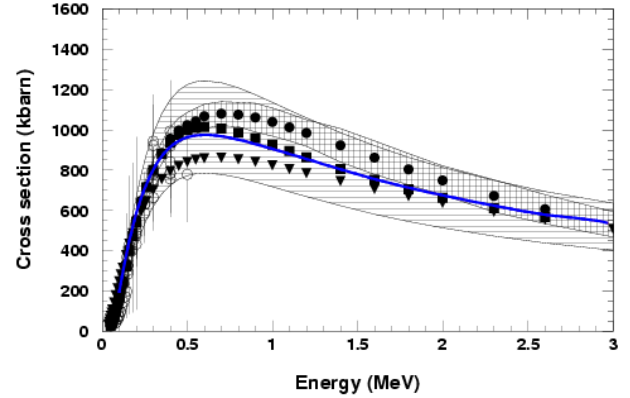


Fig. 2. K shell proton ionization cross sections, C: ECPSSR model (thick line), with Hartree-Slater (dashed), United Atom (dotted) and high energy (thin line) corrections, PWBA (triangles); Paul & Sacher [42] (filled circles) and Kahoul et al. [43] (squares) empirical models, experimental data from [42] (empty circles). Shaded bands represent Kahoul et al. (horizontal) and Paul and Sacher (vertical) uncertainties. Overlapping curves may not be visible.

From this analysis one can conclude that the implemented K shell ionization cross section models exhibit a satisfactory accuracy with respect to experimental measurements.

B. L shell ionization cross sections

The cross sections for L sub-shell ionization cross sections were compared to the experimental data collected in two complementary compilations [49], [50]. An example of how the simulation models reproduce experimental measurements is shown in Fig. 3.

The same method was applied as described for the validation of K shell cross sections.

The ECPSSR model appears to provide a satisfactory representation of L shell ionisation cross sections with respect to experimental data, especially with its United Atom variant.

The ECPSSR-UA exhibits the best overall accuracy among the various models; the Orlic et al. model exhibits the worst accuracy with respect to experimental data. This semi-empirical model is the only option implemented in Geant4 9.2 for the calculation of L shell ionization cross sections.

The accuracy of the various cross section models was studied by means of contingency tables to evaluate their differences quantitatively. The categorical analysis was performed between the ECPSSR model with United Atom correction, i.e. the model showing the best accuracy according to the results of the χ^2 test, and the other cross section models. The contingency tables were built based on the results of the χ^2 test at the 95% confidence level, summing the “pass” and “fail” outcome over the three sub-shells.

The Orlic et al. semi-empirical model is found to be significantly less accurate than the ECPSSR-UA model: the hypothesis of equivalence of their accuracy with respect to experimental data is rejected at 99% confidence level. The p-values concerning the comparison of the Miyagawa et al. empirical model are close to the critical region for 95% confidence, and slightly different for the three tests performed on the related contingency table. The Sow et al. empirical

TABLE I

PERCENTAGE OF TEST CASE WITH COMPATIBILITY AT CONFIDENCE LEVEL CL BETWEEN SIMULATION MODELS AND EXPERIMENTAL DATA OF K SHELL IONIZATION BY PROTONS

CL	ECPSSR	ECPSSR-HE	ECPSSR-HS	ECPSSR-U	Paul-Sacher	Kahoul
All measurements						
95%	67	74	77	68	71	46
99%	85	83	83	85	80	57
Excluding high energy data						
95%	69	75	86	69	70	48
99%	83	81	91	83	80	56

model and the ECPSSR model in its original formulation appears statistically equivalent in accuracy to the ECPSSR model with United Atom correction.

As a result of this analysis, the ECPSSR model with United Atom approximation can be recommended for usage in Geant4-based simulation applications as the most accurate option for L shell ionization cross sections. The ECPSSR model in its original formulation can be considered a satisfactory alternative; the Sow et al. empirical model has satisfactory accuracy, but limited applicability regards the target elements and proton energies it can handle.

C. Cross section models for high energy PIXE

PIXE as a technique for elemental analysis is usually performed with proton beams of a few MeV. In the recent years, higher energy proton beams of a few tens MeV have been effectively exploited too. High energy protons are a source of PIXE in the space radiation environment.

The interest in high energy PIXE has motivated recent theoretical investigations [38] concerning cross section calculations at higher energies. Despite the emerging interest of high energy PIXE, only a limited set of experimental data is available above the energy range of conventional PIXE techniques.

The accuracy of the implemented K shell cross section models was evaluated against two sets of measurements at higher energy [51], [52], respectively at 66 and 68 MeV. The experimental measurement with uranium was not included in the comparison, since it appears affected by some experimental systematics.

The χ^2 test was performed first separately on either experimental data set to evaluate the possible presence of any systematics in the two test cases, then on the combined data set. The p-values from the χ^2 test against these experimental data are listed in Table II.

Over the limited data sample considered in this test, the ECPSSR model with the correction in [38] this model does not appear to provide better accuracy than the original ECPSSR formulation; nevertheless more high energy experimental data would be required to reach a firm conclusion. Also, this analysis should be verified over tabulation deriving from a published version of the ISICS code, when it becomes available.

The χ^2 test over the experimental data at 160 MeV collected in [42] results in p-values less than 0.001 for all the ECPSSR model variants. The rejection of the null hypothesis could be ascribed either to the deficiency of the theory or to systematic

TABLE II

P-VALUES FROM THE χ^2 TEST CONCERNING HIGH ENERGY EXPERIMENTAL DATA

Experimental data	ECPSSR	ECPSSR HE	ECPSSR HS	ECPSSR UA
[51], 68 MeV	0.612	0.069	0.054	0.612
[52], 66 MeV	0.235	0.060	< 0.001	0.235
Combined	0.351	0.020	< 0.001	0.351

effects affecting the measurements; further data would be required for a sound assessment.

V. APPLICATION OF THE PIXE PROTOTYPE SOFTWARE

The prototype components for PIXE simulation described in the previous sections were applied to a study of the passive, graded Z shielding of the X-ray detectors of the eROSITA telescope [5] on the upcoming Russian *Spectrum-X-Gamma* space mission.

The purpose of the passive shielding is two-fold. Firstly, the passive shielding prevents abundant low-energy cosmic-ray particles from reaching the detectors and thus from causing radiation damage. Secondly, the passive graded Z shielding serves to reduce instrumental background noise to a minimum [53]. This background noise consists of both fluorescence lines and continuum background due to bremsstrahlung photons and δ rays from cosmic-ray interactions.

The event timing accuracy of current imaging Si detectors for X-ray astronomy (photon energy range $\sim 0.1 - 15$ keV) is limited by the signal integration time of these devices. For such detectors, an active anti-coincidence system cannot be used for background reduction because discarding complete readout frames correlated with an anti-coincidence signal would result in unacceptable dead time. Detector triggers due to primary cosmic-ray particles can be discriminated in imaging detectors due to their high energy deposit and their pixel image pattern. However, interactions of primary cosmic-ray particles in the detector and surrounding passive material give rise to secondary X-rays and charged particles. These may in turn lead to detector triggers within the accepted energy range. Such triggers contribute to the instrumental background noise because they cannot be distinguished from valid events due to cosmic X-ray photons that were focused by the telescope mirror system onto the detector.

The production of secondary photons and particles by the ubiquitous cosmic radiation is inevitable, but graded Z shielding permits the shifting of the energy of secondaries from atomic deexcitation to low values. The probability that an

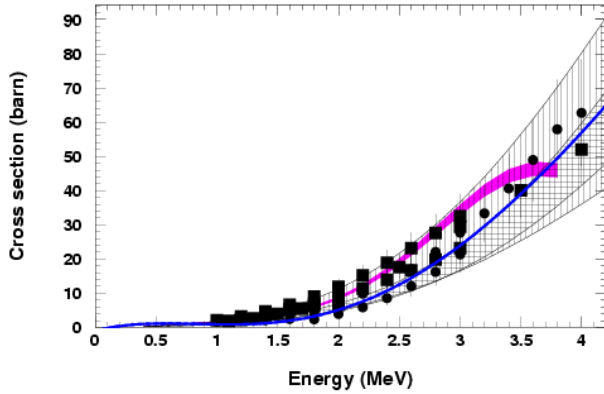
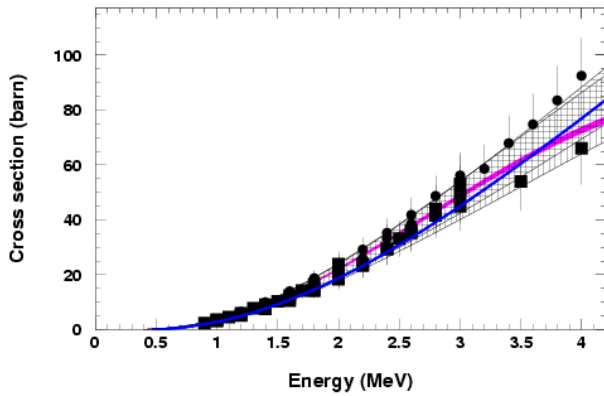
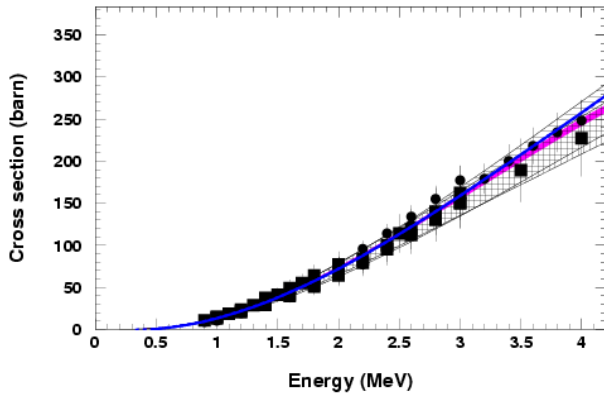
(a) L₁(b) L₂(c) L₃

Fig. 3. L sub-shell proton ionization cross sections for $Z=79$: ECPSSR model (solid line) and ECPSSR with United Atom correction (dashed line); empirical models by Miyagawa et al. (vertical shaded band), Orlic et al. (horizontal shaded band) and Sow et al. (solid shaded green band); experimental data from [49] (squares) and [50] (circles). Shaded bands represent model uncertainties. Overlapping curves may not be visible.

atomic shell vacancy is filled by radiative transitions (emission of fluorescence X-ray photons) decreases with decreasing atomic charge number Z ; by contrast, the probability for non-radiative transitions (emission of Auger and Coster-Kronig electrons) increases. The average energy of secondaries from atomic deexcitation decreases with decreasing charge number Z . Therefore, in a graded Z shield cosmic-ray induced fluorescence X rays produced in an outer, higher Z layer of the shield are absorbed in an inner, lower Z layer. Subsequent atomic deexcitation in this inner layer gives rise to fluorescence photons and Auger electrons with energies that are lower than the energies of the deexcitation particles from the outer layer; in addition, there will be relatively more deexcitation electrons than X-rays. If the effective charge number Z of the innermost shield layer is sufficiently low, ionization results in the generation of mainly Auger electrons with energies below 1 keV, which can easily be stopped in a thin passivation layer on top of the detectors. Ionization can also create rare fluorescence X rays of similarly low energy.

A first set of graded Z shield designs was studied by Monte Carlo simulation, using the PIXE prototype software together with Geant4 versions 9.1-patch 01. The detector chip was modelled as a $450 \mu\text{m}$ thick square slab of pure Si with dimensions $5.6 \text{ cm} \times 3.7 \text{ cm}$. The sensitive detector, which is integrated into the chip, covers an area of $2.88 \text{ cm} \times 2.88 \text{ cm}$ or 384×384 square pixels of size $75 \mu\text{m} \times 75 \mu\text{m}$. This detector model was placed inside a box-shaped shield; figures of the actual design can be found in [54]. In its simplest form, the passive shield consisted only of a single 3 cm thick layer of pure Cu; the outer dimensions of the shield were $12.7 \text{ cm} \times 10.8 \text{ cm} \times 7.1 \text{ cm}$. A second version of the graded Z shield had a 1 mm thick Al layer inside the Cu layer, and a third version in addition a 1 mm thick B_4C layer inside the Al layer. The physics configuration in the simulation application involved the library-based processes of the Geant4 low energy electromagnetic package for electrons and photons, along with the improved version of the hadron ionisation process and the specific PIXE software described in section III. Among the ionization cross section models, the ECPSSR ones were selected for K, L and M shells.

Spectrum-X-Gamma is expected to be launched in 2012 into an L2 orbit. The background spectra due to cosmic-ray protons were simulated for the three different eROSITA graded Z shield designs. A model for the detector response, taking into account Fano statistics (and hence the energy resolution) and detector noise, was then applied to obtain a simulated data sets. These simulated data were further processed with specialized data analysis algorithms [55]. A comparison of the results is depicted in Fig. 4. The spectra represent the average background in a detector pixel. Qualitatively, the PIXE prototype implementation is working properly: protons produce the expected fluorescence lines with correct relative strengths. In case of a pure Cu shield, shown in Fig. 4(a), strong Cu K_α and K_β fluorescence lines at about 8.0 and 8.9 keV are present in the background spectrum. In case of a combined Cu-Al shield, depicted in Fig. 4(b), the Cu fluorescence lines are absorbed in Al, but ionization in Al gives rise to a clear Al K_α fluorescence line at about 1.5 keV.

In case of the full graded Z shield configuration, shown in Fig. 4(c), the B_4C layer absorbs the Al line, but at the same is not a source of significant fluorescence lines, which is expected due to the low fluorescence yield of these light elements.

Except for an excess below 0.3 keV for the case of the Cu-Al- B_4C graded Z shield, which appears because the simulated detector model does not yet include a thin passivation layer, there is no significant difference in the continuum background for the three different designs. The inclusion of a thin layer for the treatment of the low energy background will be the object of a further detector design optimization.

This application demonstrates that the developed software is capable of supporting concrete experimental studies. Nevertheless, the concerns outlined in sections II-B and III-B should be kept in mind: while the present PIXE simulation component can provide valuable information in terms of relative fluorescence yields from inner shells, the intrinsic limitations of the mixed transport scheme in which ionization is modelled and the lack of cross section calculations for outer shells prevent an analysis of the simulation outcome in absolute terms. .

VI. CONCLUSION AND OUTLOOK

This paper presents a brief overview of the status, open issues and recent developments of PIXE simulation with Geant4; a more extensive report of the underlying concepts, developments and results is available in [56].

These new developments represent a significant step forward regards PIXE simulation with Geant4. They extend the capabilities of the toolkit by enabling the generation of PIXE associated with K, L and M shells for protons and α particles; for this purpose a variety of cross section models are provided. The adopted data-driven strategy and the software design improve the computational performance over previous Geant4 models. The validity of the implemented models has been quantitatively estimated with respect to experimental data.

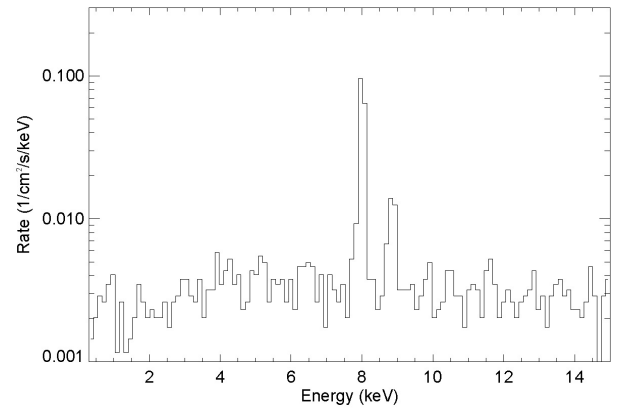
An extensive ionisation cross section data library has been created as a by-product of the development process: it can be of interest to the experimental community for a variety of applications, not necessarily limited to PIXE simulation with Geant4.

Some issues identified in the course of the development process are still open: they concern the consistency of PIXE simulation in a mixed condensed-discrete particle transport scheme. In parallel, a project [57] is in progress to address design issues concerning co-working condensed and discrete transport methods in a general purpose simulation system.

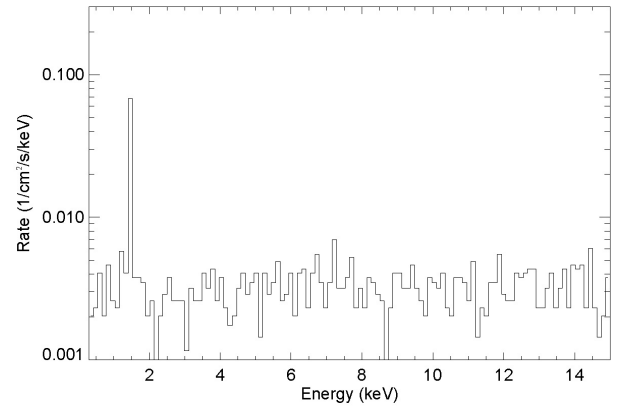
Despite the known limitations related to mixed transport schemes, the software developments described in this paper provide sufficient functionality for realistic experimental investigations.

ACKNOWLEDGMENT

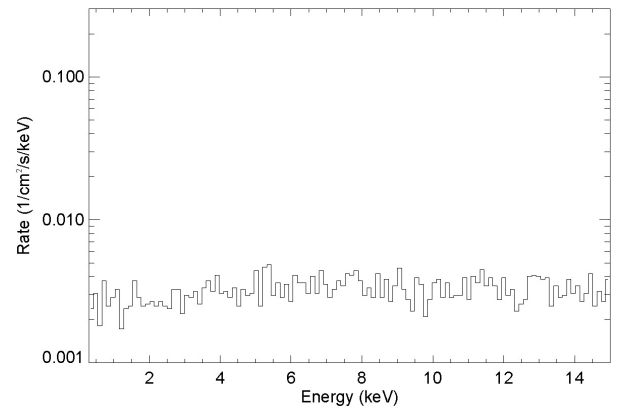
The authors express their gratitude to A. Zucchiatti for valuable discussions on PIXE experimental techniques and to S. Cipolla for providing a prototype version of ISICS including updates for high energy K shell cross sections.



(a) Cu Shield



(b) Cu-Al Shield



(c) Cu-Al- B_4C Shield

Fig. 4. A comparison of the fluorescence background due to ionization by cosmic-ray protons in an L2 orbit for three different graded Z shield designs for the eROSITA X-ray detectors.

The authors are grateful to the RSICC staff, in particular B. L. Kirk and J. B. Manneschildt, for the support to assemble a ionization cross section data library resulting from the developments described in this paper.

REFERENCES

- [1] T. B. Johansson et al., "X-ray analysis: elemental trace analysis at the 10^{-12} g level", *Nucl. Instrum. Meth.*, vol. 84, no. 1, pp. 141-143, 1970.
- [2] S. A. E. Johansson et al., "Particle-induced X-ray Emission Spectrometry (PIXE)", Wiley-Interscience, New York, 1995.

- [3] S. Agostinelli et al., "Geant4 - a simulation toolkit" *Nucl. Instrum. Meth. A*, vol. 506, no. 3, pp. 250-303, 2003.
- [4] J. Allison, et al., "Geant4 Development and Applications", *IEEE Trans. Nucl. Sci.*, vol. 53, no. 1, pp. 270-278, 2006.
- [5] P. Predehl et al., "eROSITA", in *Proc. of the SPIE*, vol. 6686, pp. 668617-668617-9, 2007.
- [6] P. Murdin, "Spectrum-X Gamma", in *Encyclopedia Astron. Astrophys.*, Bristol: Inst. of Physics Publishing, 2001.
- [7] C. G. Ryan et al., "Quantitative analysis of PIXE spectra in geoscience applications", *Nucl. Instrum. Meth. B*, vol. 49, no. 1-4, pp. 271-276, 1990.
- [8] J. A. Maxwell et al., "The Guelph PIXE software package", *Nucl. Instrum. Meth. B*, vol. 43, no. 2, pp. 218-230, 1989.
- [9] J. A. Maxwell et al., "The Guelph PIXE software package II", *Nucl. Instrum. Meth. B*, vol. 95, no. 3, pp. 407-421, 1995.
- [10] J. L. Campbell et al., "The Guelph PIXE software package III: Alternative proton database" *Nucl. Instrum. Meth. B*, vol. 170, pp. 193-204, 2000.
- [11] E. Clayton, "PIXAN, the Lucas Heights PIXE analysis computer package", ANSTO. AAEC/M113, 1986.
- [12] G. Szabo and I. Borbely-Kiss, "PIXYKLM computer package for PIXE analyses" *Nucl. Instrum. Meth. B*, vol. 75, no. 1-4, pp. 123-126, 1993.
- [13] K. Sera and S. Futatsugawa, "Personal computer aided data handling and analysis for PIXE", *Nucl. Instrum. Meth. B*, vol. 109-110, pp. 99-104, 1996.
- [14] B. Vekemans et al., "Analysis of X-ray Spectra by Iterative Least Squares (AXIL): New Developments", *X-ray spectrometry*, vol. 23, no. 6, pp. 278-285, 1994.
- [15] A.D. Lipworth et al., "Advanced, enhanced HEX program for PIXE", *Nucl. Instrum. Meth. B*, vol. 75, no. 1-4, pp. 127-130, 1993.
- [16] K. K. Loh et al., "Computer simulation of PIXE and μ -PIXE spectra for inhomogeneous thick target analysis", *Nucl. Instrum. Meth. B*, vol. 77, no. 1-4, pp. 132-136, 1993.
- [17] I. Orlic et al., "Virtual PIXE and RBS laboratory", *Nucl. Instrum. Meth. B*, vol. 150, no. 1-2, pp. 83-89, 1999.
- [18] C. Pascual-Izarra et al., "LibCPIXE: A PIXE simulation open-source library for multilayered samples", *Nucl. Instrum. Meth. B*, vol. 249, pp. 820-822, 2006.
- [19] W. Brandt and G. Lapicki, "Energy-loss effect in inner-shell Coulomb ionization by heavy charged particles", *Phys. Rev. A*, Vol. 23, 1717, 1981.
- [20] Y. Namito and H. Hirayama, "Implementation of electron-impact ionization into the EGS4 code" *Nucl. Instrum. Meth. A*, vol. 423, no. 2-3, pp. 238-246, 1999.
- [21] I. Kawrakow and D.W.O. Rogers, "The ENSrc Code System: Monte Carlo Simulation of Electron and Photon Transport", NRCC Report PIRS-701, Sep. 2006.
- [22] H. Hirayama, et al., "The EGS5 code system", Report SLAC-R-730, Stanford Linear Accelerator Center, Stanford, CA, USA, 2006.
- [23] J. Baro et al., "PENELOPE: An algorithm for Monte Carlo simulation of the penetration and energy loss of electrons and positrons in matter" *Nucl. Instrum. Meth. B*, vol. 100, no. 1, pp. 31-46, 2005.
- [24] M. J. Berger, "Monte Carlo calculation of the penetration and diffusion of fast charged particles", in *Methods in Computational Physics*, vol. 1, Ed. B. Alder, S. Fernbach and M. Rotenberg, Academic Press, New York, pp. 135-215, 1963.
- [25] S. T. Perkins, D. E. Cullen, and S. M. Seltzer, "Tables and Graphs of Electron-Interaction Cross Sections from 10 eV to 100 GeV Derived from the LLNL Evaluated Electron Data Library (EEDL)", UCRL-50400 Vol. 31, 1997.
- [26] S. Saliceti, "Studio della Composizione del Pianeta Mercurio: Modelli per l'Emissione di Fluorescenza e la loro Validazione Sperimentale", MSc. Thesis, Univ. of Genova, 2004.
- [27] S. Guatelli et al., "Geant4 Atomic Relaxation", in *Conf. Rec. 2004 IEEE Nucl. Sci. Symp.*, pp. 2178-2181, 2004.
- [28] A. Mantero et al., "Geant4 Atomic Relaxation Models", in *The Monte Carlo Method: Versatility Unbounded in a Dynamic Computing World*, on CD-ROM, American Nuclear Society, LaGrange Park, IL, 2005.
- [29] A. Mantero, "Development and validation of X-ray fluorescence simulation models for planetary astrophysics investigations", PhD Thesis, Univ. of Genova, 2008.
- [30] M. Gryziński, "Two-Particle Collisions. I. General Relations for Collisions in the Laboratory System", *Phys. Rev.*, vol. 138, 2A, pp. 305-322, 1965.
- [31] M. Gryziński, "Two-Particle Collisions. II. Coulomb Collisions in the Laboratory System of Coordinates", *Phys. Rev.*, vol. 138, 2A, pp. 322-335, 1965.
- [32] H. Abdelhawahed et al., "New Geant4 Cross Section Models for PIXE Simulation", *Nucl. Instrum. Meth. B*, vol. 267, no. 1, pp. 37-44, 2009.
- [33] G. Weidenspointner et al., "Application of the Geant4 PIXE implementation for space missions - new models for PIXE simulation with Geant4" in *Conf. Rec. 2008 IEEE Nucl. Sci. Symp.*, pp. 2877-2884.
- [34] S. Guatelli et al., "Geant4 Atomic Relaxation", *IEEE Trans. Nucl. Sci.*, vol. 54, no. 3, pp. 585-593, 2007.
- [35] G. Booch, J. Rumbaugh, and I. Jakobson, "The Unified Modelling Language User Guide", Ed. Boston: Addison-Wesley, 1999.
- [36] S. J. Cipolla, "The united atom approximation option in the ISICS program to calculate K, L, and M-shell cross sections from PWBA and ECPSR theory", *Nucl. Instrum. Meth. B*, vol. 261, pp. 142-144, 2007.
- [37] G. Lapicki, "The status of theoretical K-shell ionization cross sections by protons", *X-Ray Spectrom.*, vol. 34, pp. 269-278, 2005.
- [38] G. Lapicki, "Scaling of analytical cross sections for K-shell ionization by nonrelativistic protons to cross sections by protons at relativistic velocities", *J. Phys. B*, vol. 41, pp. 115201, 2008.
- [39] Z. Liu and S.J. Cipolla, "ISICS: A program for calculating K, L, and M-shell cross sections from ECPSR theory using a personal computer", *Comp. Phys. Comm.*, vol. 97, pp. 315-330, 1996.
- [40] S. J. Cipolla, "An improved version of ISICS: a program for calculating K, L, and M-shell cross sections from PWBA and ECPSR theory using a personal computer", *Comp. Phys. Comm.*, vol. 176, pp. 157-159, 2007.
- [41] S. Cipolla, ISICS, 2008 version. Private communication: S. Cipolla, Creighton Univ., Omaha NE 68178.
- [42] H. Paul and J. Sacher, "Fitted empirical reference cross sections for K-shell ionization by protons", *At. Data Nucl. Data Tab.*, vol. 42, pp. 105-156, 1989.
- [43] A. Kahoul, M. Nekkab, and B. Deghfel, "Empirical K-shell ionization cross-sections of elements from 4Be to 92U by proton impact", *Nucl. Instrum. Meth. B*, vol. 266, pp. 4969-4975, 2008.
- [44] H. Paul and O. Bolik, "Fitted Empirical Reference Cross Sections for K-Shell Ionization by Alpha Particles", *At. Data Nucl. Data Tab.*, vol. 54, pp. 75-131, 1993.
- [45] Y. Miyagawa et al., "Analytical Formulas for Ionization Cross Sections and Coster-Kronig Corrected Fluorescence Yields of the L₁, L₂, and L₃ Subshells", *Nucl. Instrum. Meth. B*, vol. 30, pp. 115-122, 1988.
- [46] C. H. Sow et al., "New parameters for the calculation of L subshell ionization cross sections", *Nucl. Instrum. Meth. B*, vol. 75, pp. 58-62, 1993.
- [47] I. Orlic et al., "Semiempirical Formulas for Calculation of L Subshell Ionization Cross Sections", *Int. J. PIXE*, vol. 4, no. 4, pp. 217-230, 1994.
- [48] R. A. Fisher, "On the interpretation of χ^2 from contingency tables, and the calculation of P", *J. Royal Stat. Soc.*, vol. 85, no. 1, pp. 87-94, 1922.
- [49] R. S. Sokhi and D. Crumpton, "Experimental L-Shell X-Ray Production and Ionization Cross Sections for Proton Impact", *At. Data Nucl. Data Tab.*, vol. 30, pp. 49-124, 1984.
- [50] I. Orlic et al., "Experimental L-shell X-ray production and ionization cross sections for proton impact", *At. Data Nucl. Data Tab.*, vol. 56, pp. 159-210, 1994.
- [51] A. Denker et al., "High-energy PIXE using very energetic protons: quantitative analysis and cross-sections", *X-Ray Spectrom.*, vol. 34, no. 4, pp. 376-380, 2005.
- [52] M. Peisach and C. A. Pineda, "Prompt analysis of heavy elements by high-energy-induced (p, X) reactions", *Nucl. Instrum. Meth. A*, vol. 299, no. 1-3, pp. 618-623, 1990.
- [53] E. Pfeiffermann et al., "Shielding of cosmic ray induced background in CCD detectors for X-ray astronomy", *Proc. SPIE*, vol. 5501, pp. 304-311, 2004.
- [54] N. Meidinger et al., "eROSITA camera design and first performance measurements with CCDs", in "Space Telescopes and Instrumentation 2008: Ultraviolet to Gamma Ray", *Proc. SPIE*, vol. 7011, 70110J, 2008.
- [55] R. Andritschke et al., "Data Analysis for Characterizing pnCCDs", in *Conf. Rec. 2008 IEEE Nucl. Sci. Symp.*, pp. 2166-2172, 2008.
- [56] M. G. Pia et al., "PIXE simulation with Geant4", *IEEE Trans. Nucl. Sci.*, vol. 56, no. 6, Dec. 2009.
- [57] M. Augelli et al., "Geant4-related R&D for new particle transport methods", in *Conf. Rec. 2009 IEEE Nucl. Sci. Symp.*